

See discussions, stats, and author profiles for this publication at: <https://www.researchgate.net/publication/236272489>

# Image denoising based on non-local means filter and its method noise thresholding

Article in *Signal Image and Video Processing* · November 2013

DOI: 10.1007/s11760-012-0389-y

---

CITATIONS

142

READS

8,161

1 author:



Shreyamsha Kumar B. K.

Concordia University

38 PUBLICATIONS 1,637 CITATIONS

SEE PROFILE

# IMAGE DENOISING BASED ON NON LOCAL-MEANS FILTER AND ITS METHOD NOISE THRESHOLDING

---

B. K. Shreyamsha Kumar

© Springer-Verlag London Limited 2012. All rights reserved.

This paper was published in Springer's Signal, Image and Video Processing Journal and the original publication is available at [www.springerlink.com](http://www.springerlink.com) (DOI: [10.1007/s11760-012-0389-y](https://doi.org/10.1007/s11760-012-0389-y)). Permission to make digital or hard copies of all or part of this work for personal or classroom use is granted without fee provided that copies are not made or distributed for profit or commercial advantage and that copies bear this notice and the full citation on the first page. Systematic or multiple reproduction, distribution to multiple locations via electronic or other means, duplication of any material in this paper for commercial purposes, or modification of the content of the paper are prohibited and require prior specific permission and/or a fee.

Cite this article as:

B. K. Shreyamsha Kumar, "Image Denoising based on Non Local-means Filter and its Method Noise Thresholding", *Signal, Image and Video Processing*, Vol. 7, Issue 6, pp. 1211-1227, 2013,  
DOI: [10.1007/s11760-012-0389-y](https://doi.org/10.1007/s11760-012-0389-y)

## IMAGE DENOISING BASED ON NON LOCAL-MEANS FILTER AND ITS METHOD NOISE THRESHOLDING

B. K. Shreyamsha Kumar<sup>1</sup>

Central Research Laboratory, Bharat Electronics,  
Bangalore-560013, INDIA

E-Mail: shreyamsha@yahoo.com

Phone: +91-80-28381125, Fax: +91-80-28381168

### ABSTRACT

*Non local-means filter uses all the possible self-predictions and self-similarities the image can provide to determine the pixel weights for filtering the noisy image, with the assumption that the image contains an extensive amount of self-similarity. As the pixels are highly correlated and the noise is typically independently and identically distributed, averaging of these pixels results in noise suppression thereby yielding a pixel that is similar to its original value. The non local-means filter removes the noise and cleans the edges without losing too many fine structure and details. But as the noise increases, the performance of non local-means filter deteriorates and the denoised image suffers from blurring and loss of image details. This is because, the similar local patches used to find the pixel weights contains noisy pixels. In this paper, the blend of non local-means filter and its method noise thresholding using wavelets is proposed for better image denoising. The performance of the proposed method is compared with wavelet thresholding, bilateral filter, non local-means filter, multi-resolution bilateral filter. It is found that, performance of proposed method is superior to wavelet thresholding, bilateral filter and non local-means filter and superior/akin to multi-resolution bilateral filter in terms of method noise, visual quality, PSNR and Image Quality Index.*

**Keywords:** Non Local-means Filter, Bilateral Filter, Method Noise, Wavelet Thresholding, BayesShrink, Multi-resolution Bilateral Filter, Image Quality Index.

### 1. INTRODUCTION

Many scientific data sets are contaminated by noise because of data acquisition process and/or transmission, which can degrade the signal of interest. A first pre-processing step in analyzing such data sets is denoising, that is, estimating the signal of interest from the available noisy data [1].

Eventhough denoising has long been a focus of research, there always remains room for improvement, especially in image denoising. For images, noise suppression/reduction is a delicate and a difficult task because, there is a trade-off between noise reduction and preservation of actual image features. If high frequency noise is to be removed from the corrupted image, the simple spatial filtering may be sufficient, but at the cost of computational complexity involved in performing the convolution. This can be reduced by Frequency-domain methods where convolution is transformed into multiplication of the spectra due to Fourier convolution property. As the noise is spread across all frequencies, the frequency-based

---

<sup>1</sup> Department of Electrical and Computer Engineering,  
Concordia University, 1515 St.Catherine West,  
Montreal, Quebec, Canada H3G 2W1

denoising methods adopt low-pass filtering to suppress most of high-frequency components in order to denoise the image. However, this is generally not effective as it suppresses both noise as well as other high-frequency features of the image resulting in an overly smoothed denoised image.

Many of the denoising methodologies and strategies [2–13] devise a model for the noise and/or for the original signal in a suitable subspace where the differences between them are accentuated based on the following observations: (i) the noise and clean signal show different behaviors in multiresolution representation, (ii) significant geometrical components of an image (edges) or time structures of a signal (sharp transitions) over-exceed noise information, especially at low resolutions [14]. Hence, in last two decades, a flurry of research has involved the use of the wavelet transform for denoising because of its multiresolution and energy compaction properties [15, 16]. The motivation is that the small wavelet coefficients in high-frequency bands that are more likely due to noise are thresholded, leaving the large wavelet coefficients which are more likely due to signal features [10,11]. The influential works on signal denoising via wavelet thresholding or shrinkage of Donoho and Johnstone [10, 11] in the additive white Gaussian noise setting have shown that various thresholding schemes for denoising have near-optimal properties in the minmax sense and perform well in simulation studies of one-dimensional curve estimation. The main assumption in wavelet thresholding is the signal magnitudes increasingly dominate the magnitudes of the noise in a wavelet representation with increasing level, so that wavelet coefficients can be set to zero if their magnitudes are less than a predetermined threshold.

Hard-thresholding and soft-thresholding are the most popular thresholding schemes used for denoising, where the former leaves the magnitudes of coefficients unchanged if they are larger than a given threshold, while the latter just shrinks them to zero by the threshold value otherwise it is set to zero in both cases. Further, the performances of these methods are close to that of an ideal coefficient selection method if the coefficients of the underlying signal are known in advance [10, 11]. Even though soft-thresholding introduces more error or bias than hard-thresholding, it is more efficient in denoising. But for some classes of images hard-thresholding performs better [3]. However, the choice of a suitable threshold value is the major problem with both of these methods and most of their variants. Initially, Donoho and Johnstone have given a mechanism for finding a universal threshold value known as VisuShrink, which depends on the noise power and the signal size (number of samples in the image). This was derived by proving an asymptotically optimal upper bound on the approximation error in the limit of an arbitrary large signal size [10, 11, 17]. VisuShrink is a global thresholding scheme where a single value of threshold is applied globally to all the wavelet coefficients. As the given noisy signal may consist of some parts where the magnitudes of the signal are below the threshold and other parts where the noise magnitudes are above the given threshold, thresholding by VisuShrink will cut off parts of the signal on one hand and leave some noise untouched on the other hand. This observation has led to the idea of a non-uniform or adaptive threshold depending on the relationship between the energy distribution of the observed signal and that of the noise. The use of different thresholds for different decomposition levels and subbands seems more reasonable as the adaptive threshold accounts for variation of the local statistics of the wavelet coefficients.

An adaptive method of selecting a threshold that adapts to the data as well as minimizing the Stein Unbiased Risk Estimator (SURE) is developed by Donoho and Johnstone, which is called as SureShrink wavelet thresholding technique [10, 17]. This is achieved by choosing distinct thresholds for each subband of each decomposition level of the wavelet tree using an efficient

recursive process [2]. Eventhough the SureShrink thresholding method clearly provides an adaptive thresholding strategy; its performance depends on the estimated statistics of the wavelet coefficients of the original image from that of the noisy image. Among the literature available on threshold value selection for image denoising, BayesShrink proposed by Chang et al. [3] has a better Mean Squared Error (MSE) performance than SureShrink. This has been derived in a Bayesian framework assuming a generalized Gaussian distribution for the wavelet coefficients.

An alternative to the wavelet-based denoising methods is the Bilateral Filter (BF) introduced by Tomasi and Manduchi [18] which considers both the spatial and the intensity information between a point and its neighboring points unlike the conventional linear filtering where only spatial information is considered. The concept of the BF was earlier presented in [19] as the SUSAN filter and in [20] as the neighborhood filter. The BF takes a weighted sum of pixels in a local neighborhood; the weights depend on both the spatial distance and the intensity distance. This preserves the edges/sharp boundaries very well while noise is averaged out as it average pixels belonging to the same region as the reference pixel. But it fails when the standard deviation of the noise exceeds the edge contrast. Recently, a relation between BF and anisotropic diffusion has been established in [21]. Also, Elad [22] proved that the BF is identical to a single Jacobi iteration of a weighted least squares minimization. In the last decade, the classical BF algorithm [23-27] has been modified and improved by many researchers. In [28, 29], the authors give an empirical study of the optimal BF parameter selection in image denoising applications and proposed the Multi-Resolution Bilateral Filter (MRBF). The application of BF on the approximation subband results in loss of some image details, whereas that after each level of wavelet reconstruction flattens the gray levels thereby resulting in a cartoon-like appearance. Further, the variants of MRBF proposed in [30] for denoising of magnetic resonance images and in [31] for astronomical, ultrasound and x-ray images also suffers from loss of some image details as well as flattening of gray levels due to BF. This is because, the application of BF removes noise as well as some image details by spatial filtering without loss of edge information (range filtering). The problem of cartoon-like appearance due to flattening of gray levels is minimized by applying BF only once during the process of denoising, thereby avoiding loss of too many image details consequently improving the denoising performance [32].

Recently, Buades et al. proposed a Non Local-means (NL-means) filter [33] which systematically uses all the possible self-predictions the image can provide and similarity of local patches to determine the pixel weights. As the patch size reduces to one pixel, the NL-means filter becomes equivalent to the BF. The former better cleans the edges without losing too many fine structures and details while the later loses details and creates irregularities on the edges. Further, Kervrann et al. [34] extended the work of [33] by controlling the neighborhood of each pixel adaptively. All these denoising methods works well with less noise (high SNR) but fails to do so with more noise (low SNR). As both the target pixel and the similar local patches which are used to find the pixel weights are noisy, the estimate of NL-means filter becomes biased [35]. To cater for this problem of noisy target pixel, adaption of central kernel weight (AKW) to the degree of noise is proposed in [35]. But this does not take care of the similar noisy local patches and hence, especially at higher noise, the biased estimate degrades/blurs the image by removing much of the image details. In order to resolve these issues, an amalgamation of NL-means Filtering and its method noise thresholding using wavelets has been proposed for image denoising.

The paper is organized as follows: section 2 discusses the NL-means Filter, section 3 proposes the NL-means Filter and its method noise thresholding using wavelets for image denoising, section 4 discusses experimental results, and conclusions follow in section 5.

## 2. NL-MEANS FILTER

The goal of image denoising is to remove the noise while retaining the important image features like edges, details as much as possible. Linear filter convolves the image with a constant matrix to obtain a linear combination of neighborhood values and has been widely used for noise elimination in the presence of additive noise. This produces a blurred and smoothed image with poor feature localization and incomplete noise suppression.

Neighborhood filter, proposed by Yaroslavsky, averages only similar gray level pixels inside the spatial neighborhood  $B_\sigma(x)$  [20] and is given by

$$YNF_{h,\sigma}v(x) = \frac{1}{C(x)} \int_{B_\sigma(x)} v(y) e^{-\frac{|v(y)-v(x)|^2}{h^2}} dy \quad (1)$$

where,  $x \in$  image  $\Omega$ ,  $y \in B_\sigma(x)$ ,  $C(x) = \int_{B_\sigma(x)} e^{-\frac{|v(y)-v(x)|^2}{h^2}} dy$  is the normalization factor and  $h$  controls the pixel similarity. The Yaroslavsky filter is less known than more recent versions, namely the SUSAN filter [19] and the BF [18]. Both algorithms, instead of considering a fixed spatial neighborhood  $B_\sigma(x)$ , weigh the distance to the reference pixel  $x$ ,

$$SNF_{h,\sigma}v(x) = \frac{1}{C(x)} \int_{B_\sigma(x)} v(y) e^{-\frac{|y-x|^2}{\sigma^2}} e^{-\frac{|v(y)-v(x)|^2}{h^2}} dy \quad (2)$$

where,  $C(x) = \int_{B_\sigma(x)} e^{-\frac{|y-x|^2}{\sigma^2}} e^{-\frac{|v(y)-v(x)|^2}{h^2}} dy$  is the normalization factor and  $\sigma$  is a spatial filtering parameter. These filters maintain sharp boundaries since they average pixels belonging to the same region as the reference pixel. The problem with these filters is that comparing only grey level values around a given pixel is not so robust when these values are noisy. Further, the Neighborhood filters also create artificial shocks. In last decade, Buades et al. have extended the Neighborhood filters to a wider class which they called it as Non Local-means (NL-means) [33, 36]. This is with the assumption that the image contains an extensive amount of self-similarity and is used to find the pixel weights for filtering the noisy image. The most similar pixels to a given pixel have no reason to be close to it. Think of the periodic patterns, or the elongated edges which appear in most images. It is therefore licit to scan a vast portion of the image in search of all the pixels that really resemble the pixel to be denoised. The resemblance is evaluated by comparing a whole window around each pixel, not just the pixel value. Denoising is then done by computing the average gray value of these most resembling pixels. Since the image pixels are highly correlated while noise is typically independently and identically distributed (i.i.d.), averaging of these pixels results in noise cancellation and yields a pixel that is similar to its original value.

Given a discrete noisy image  $v = \{v(i) | i \in I\}$ , the estimated value  $NL(i)$  for a pixel  $i$ , is computed as a weighted average of all the pixel intensities  $v(j)$  in the image  $I$ ,

$$NL(i) = \sum_{j \in I} w(i,j)v(j), \quad (3)$$

where  $w(i,j)$  is the weight assigned to value  $v(j)$  for restoring the pixel  $i$ . Eventhough the traditional definition of the NL-means filter considers the intensity of each pixel can be linked to pixel intensities of the whole image, for practical and computational considerations, the number of pixels taken into account in the weighted average is restricted to a neighborhood search window  $S_i$  centered at the pixel  $i$ . More precisely, the weight  $w(i,j)$  evaluates the similarity between the intensities of the local neighborhoods (patches)  $v(N_i)$  and  $v(N_j)$

centered on pixels  $i$  and  $j$ , such that  $0 \leq w(i,j) \leq 1$  and  $\sum_j w(i,j) = 1$ , where  $N_k$  denotes a square neighborhood of fixed size centered at a pixel  $k$  and is within the search window  $S_i$  centered at the pixel  $i$ . This similarity is measured as a decreasing function of the weighted Euclidean distance,  $\|v(N_i) - v(N_j)\|_{2,\sigma}^2$ , where  $\sigma > 0$  is the standard deviation of the Gaussian kernel. This distance is the traditional  $L_2$ -norm convolved with a Gaussian kernel of standard deviation  $\sigma$ . Indeed in digital images, closer pixels are more dependent and therefore closer pixels to the central one should have more importance in the window comparison. Hence, the Gaussian kernel is used to assign spatial weights to the pixels in the window such that the central pixel in the window contribute more to the distance than the pixels located at the periphery. The weights  $w(i,j)$  are computed as follows:

$$w(i,j) = \frac{1}{Z(i)} e^{-\frac{\|v(N_i) - v(N_j)\|_{2,\sigma}^2}{h^2}} \quad (4)$$

where  $Z(i)$  is a normalization constant

$$Z(i) = \sum_j e^{-\frac{\|v(N_i) - v(N_j)\|_{2,\sigma}^2}{h^2}} \quad (5)$$

ensuring that  $\sum_j w(i,j) = 1$  and  $h$  is the smoothing kernel width which controls the decay of the exponential function and therefore the decay of the weights as a function of the Euclidean distances. From Eq. (5), it can be seen that a small  $h$  shrinks the area of averaging and thus noise is not likely to be suppressed enough. Conversely, if  $h$  is too large, the weights at the boundary of  $S_i$  are also very large, which results in blurry output. Further, due to the fast decay of the exponential kernel, large Euclidean distances lead to nearly zero weights acting as an automatic threshold. Since the NL-means filter not only compares the grey level in a single point but also the geometrical configuration in a whole neighborhood, it allows a more robust comparison than neighborhood filters.

The application of the Euclidean distance to the noisy neighborhoods raises the following equality

$$E\|v(N_i) - v(N_j)\|_{2,\sigma}^2 = \|u(N_i) - u(N_j)\|_{2,\sigma}^2 + 2\sigma_n^2 \quad (6)$$

where  $u$  denotes the original (unknown) image and  $v$  the noisy image obtained by adding a white noise. This equality shows the robustness of the algorithm since in expectation the Euclidean distance conserves the order of similarity between pixels. Thus, using a threshold function and setting this hard threshold to  $2\sigma_n^2$  leads to take an average of pixels which originally had an almost identical window around them.

### 3. NL-MEANS FILTER AND ITS METHOD NOISE THRESHOLDING

The image denoising framework using the blend of NL-means Filter and its Method noise Thresholding using wavelets (NLFMT) is shown in Fig. 1. A difference between the original image and its denoised image shows the noise removed by the algorithm, which is called as method noise. In principle, the method noise should look like a noise. Since even good quality images have some noise, it makes sense to evaluate any denoising method in that way, without the traditional “add noise and then remove it” trick. Mathematically, it is given by

$$MN = A - I_F \quad (7)$$

where,  $A$  is the original image (not necessarily noisy) and  $I_F$  is the output of denoising operator for a input image  $A$ .

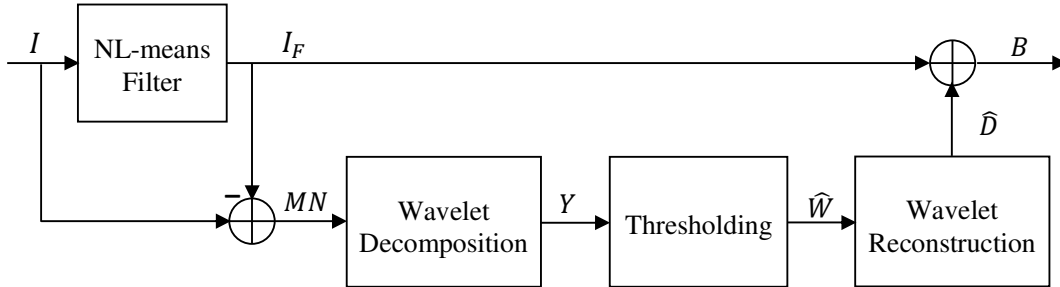


**Fig. 1** Proposed Image Denoising Framework

The application of NL-means filter on the noisy image removes the noise and cleans the edges without losing too many fine structures and details. Eventhough the NL-means filter is very effective in removing the noise at high SNR (with less noise) but as the noise increases, its performance deteriorates. This is because; the similar local patches which are used to find the pixel weights are also noisy. To capture what is removed from the noisy image by the NL-means filter, the definition of the method noise is redefined as the difference between the noisy image and its denoised image. Hence, Eqn. (7) is rewritten as

$$MN = I - I_F \quad (8)$$

where,  $I = A + Z$  is a noisy image obtained by corrupting the original image  $A$  by a white Gaussian noise  $Z$  and  $I_F$  is the output of NL-means filter for a input image  $I$ .

At low SNR, the NL-means filter not only removes the noise but at the same time it blurs the image thereby removing much of the image details. Consequently, the method noise will consists of noise as well as image details along with some edges. Hence, the method noise  $MN$  can be considered as a combination of image details  $D$  and a white Gaussian noise  $N$  and is written as [32]

$$MN = D + N \quad (9)$$

Now the problem is to estimate the detail image  $D$ , which has only the original image features and edges/sharp boundaries that are removed by NL-means filter, as accurately as possible according to some criteria and is added with the NL-means filtered image  $I_F$  to get better denoised image with details. In wavelet domain, Eqn. (9) can be represented as

$$Y = W + N_w \quad (10)$$

where  $Y$  is the noisy wavelet coefficient (method noise),  $W$  is the true wavelet coefficient (detail image) and  $N_w$  is independent Gaussian noise.

In wavelet domain, the goal is to estimate the true wavelet coefficient  $W$  from  $Y$  by thresholding  $Y$  with a proper value of threshold which minimizes MSE so that it can retain the original image features and edges/sharp boundaries very well in the final denoised image. The estimate of the true wavelet coefficient is represented as  $\widehat{W}$  and its wavelet reconstruction gives an estimate of detail image  $\widehat{D}$ . The summation of this detail image  $\widehat{D}$  with the NL-means filtered image  $I_F$  will give the denoised image  $B$ , certainly have more image details and edges as compared with NL-means filtered image  $I_F$ .

The wavelet thresholding adds power to the proposed method as noise components can be eliminated better in detail subbands of method noise. The adaptive method of selecting a threshold developed by Donoho and Johnstone, minimizes the Stein Unbiased Risk Estimator (SURE) [37], which has been known as the SureShrink wavelet thresholding technique [10, 17]. The adaptivity of SureShrink is achieved by choosing distinct thresholds for each subband of each level of the wavelet tree using an efficient recursive process [2, 3]. This thresholding

scheme attempts to select thresholds that adapt to the data as well as minimize an estimation of the MSE or risk. Further, it uses a hybrid approach while selecting the SURE threshold or local universal threshold depending on the energy of a particular subband. That is, it uses SURE threshold in high activity subbands and localized universal threshold in sparse subbands. Although the SureShrink thresholding method clearly provides an adaptive thresholding strategy, its performance is dependent on estimating the statistics of the wavelet coefficients of the original image from that of the noisy image. In last decade, there has been a fair amount of research on threshold value selection for image denoising. Among them, Chang et al. have proposed a BayesShrink method which derives a threshold in a Bayesian framework assuming a generalized Gaussian distribution for the wavelet coefficients [3]. This method has a better MSE performance than SureShrink and hence, it is used in the proposed method to threshold the method noise wavelet coefficients.

BayesShrink is also an adaptive, data-driven thresholding strategy via soft-thresholding which derives the threshold in a Bayesian framework, assuming a generalized Gaussian distribution. This method is adaptive to each sub-band because it depends on data-driven estimates of the parameters. The threshold for a given subband derived by minimizing Bayesian risk, given by

$$T = \frac{\sigma_n^2}{\sigma_w} \quad (11)$$

where  $\sigma_n^2$  is the noise variance estimated from subband  $\text{HH}_1$  by a robust median estimator [3], given by

$$\hat{\sigma}_n = \frac{\text{Median}(|Y_{i,j}|)}{0.6745}, \quad Y_{i,j} \in \{\text{HH}_1\} \quad (12)$$

and  $\sigma_w^2$  is the variance of wavelet coefficients in that subband, whose estimate is computed using

$$\hat{\sigma}_w^2 = \max(\hat{\sigma}_y^2 - \hat{\sigma}_n^2, 0) \quad (13)$$

where  $\hat{\sigma}_y^2 = \frac{1}{MN} \sum_{i,j=1}^{M,N} Y_{i,j}^2$ .

#### 4. RESULTS AND DISCUSSION

Experiments were carried out on various standard grayscale images of size 512 x 512 which are shown in Fig. 2. The input images are corrupted by a simulated Gaussian white noise with zero mean and five different standard deviations  $\sigma \in [10, 20, 30, 40, 50]$ . The denoising process has been performed on these five noisy realizations. To validate the superiority of the proposed method NLFMT, its performance is compared in terms of method noise, visual quality, PSNR and Image Quality Index (IQI) of the denoised images using the various methods available in literature such as Wavelet based Thresholding (WT), BF, MRBF, NL-means filter and BM3D [38]. For BM3D, the parameter values suggested by the authors are used. In all the cases, db8 is used for wavelet decomposition and BayesShrink soft thresholding is used to threshold these wavelet coefficients. In WT based thresholding and NLFMT, three levels of decomposition is used whereas in MRBF only one decomposition level is used. The other parameters used are given against the methods considered.

MRBF:  $\sigma_s = 1.8$ ,  $\sigma_r = \sigma_n$ , neighborhood window=11x11

BF:  $\sigma_s = 1.8$ ,  $\sigma_r = 5\sigma_n$ , neighborhood window=11x11

NL-means:  $\sigma_s = 5$ ,  $h = 0.55\sigma_n$ , neighborhood window=7x7, search window=21x21

NLFMT:  $\sigma_s = 5$ ,  $h = 0.55\sigma_n$ , neighborhood window=7x7, search window=21x21

The method noise of a very good image denoising method should look like a noise even for a noise free image. That is, any denoising algorithm should not alter the noise free images, so

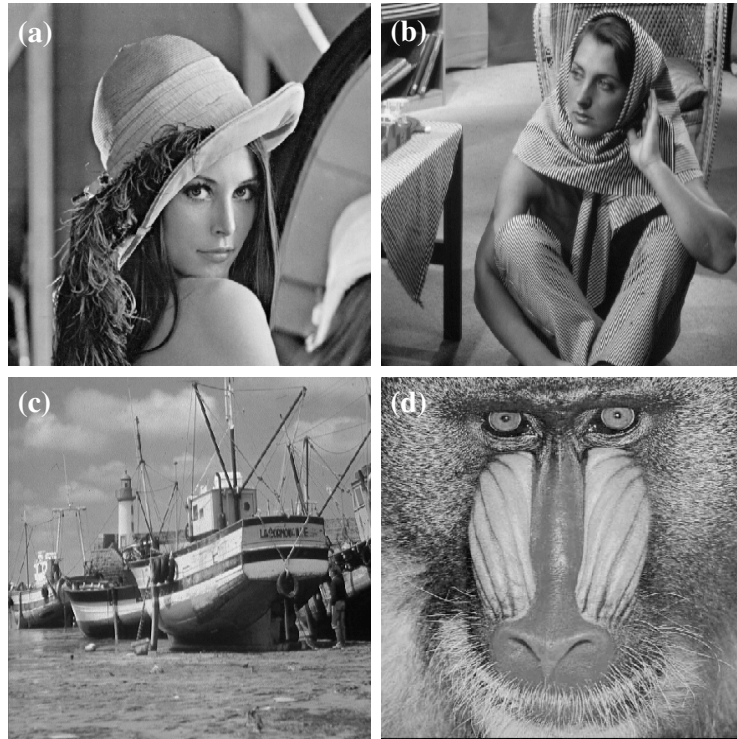


**Fig. 2** Original Images used for experiments (a) Lena, (b) Barbara, (c) Boat, (d) Baboon

that the method noise should be very small when some kind of regularity for the image is assumed. Since the removed details, texture or edges have a large method noise; it helps us to understand the performance and limitations of the denoising algorithms. Fig. 3 shows the performance of the WT, MRBF, BF, NL-means filter, proposed method (NLFMT) and BM3D in terms of method noise for an input image of boat with  $\sigma = 2.5$ . It is observed from Fig. 3 that, the method noise of WT (Fig. 3 (d)) and NLFMT (Fig. 3 (f)) looks like a noise with very minimal details whereas that of NL-means filter (Fig. 3 (c)) and MRBF (Fig. 3 (e)) has more details near the bottom of the boat. Fig. 3 (b) shows the increased details throughout the method noise image which is due to BF. The method noise of BM3D (Fig. 3(g)) looks like noise only in some portions of the image (top and bottom portion of the image) and has some image details in other regions, which is greater than that of proposed method. The wavelet thresholding of NL-means filter's method noise (Fig. 3(c)) and its addition with NL-means filter's output improve the method noise of NLFMT (Fig. 3 (f)). That is, the image details present in the method noise of NL-means filter (Fig. 3(c)) has been transferred to the denoised image of NLFMT and hence those details are not visible in the method noise of NLFMT (Fig. 3 (f)). To further explore the improvements of NLFMT over NL-means filter, the denoised images of baboon and their respective method noise  $MN$  are shown in Fig. 4 for different standard deviations  $\sigma \in [10, 20, 30]$ . With increasing noise, the NL-means filter blurs the image (beard, mouth and nose portions of baboon) (Fig. 4 (a) - (c)) and hence those details are reflected in its method noise (Fig. 4 (d) - (f)). This is not the case with NLFMT (Fig. 4 (g) - (i)) as those image details present in the method noise of NL-means filter are added to NL-means filtered output after wavelet thresholding its method noise. Hence the method noise of NLFMT looks like a noise as shown in Fig. 4 (j) - (l). In principle, the method noise should look like a noise with very small amplitudes. In order to compare the performance of the considered methods quantitatively, the minimum and maximum amplitude levels of the method noise are tabulated in Table 1. From Table 1 it is observed that, the minimum and maximum amplitudes

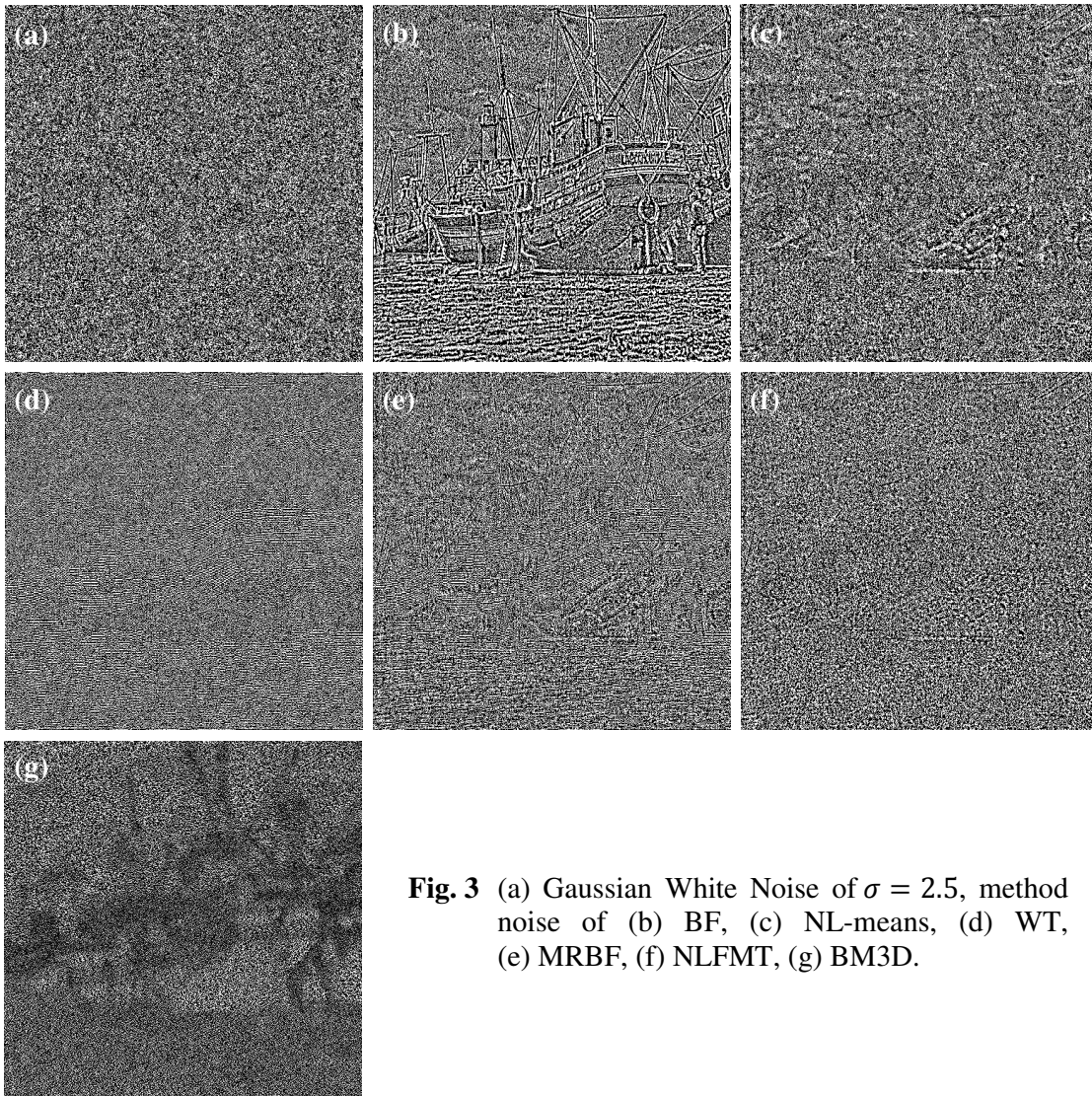


**Fig. 3** (a) Gaussian White Noise of  $\sigma = 2.5$ , method noise of (b) BF, (c) NL-means, (d) WT, (e) MRBF, (f) NLFMT, (g) BM3D.

of the method noise by BM3D stand first in the list as they have lowest value (in absolute sense) compared to other methods. This may be due to its outstanding denoising performance of BM3D. If BM3D is excluded from the comparison, then the proposed method, NLFMT, has the lesser values thereby standing second in the list (bolded in Table 1). But that of WT has higher magnitude than NLFMT and stands second in the list, which is followed by MRBF, NL-means and BF. From these observations it is found that, even though the performance of proposed method is similar/inferior to BM3D, it has shown better performance compared to other methods in terms of method noise.

Table 1 Minimum and Maximum amplitude levels of the method noise

Denoising Methods	Minimum	Maximum
WT	-22.8602	21.7308
BF	-29.5608	28.4542
MRBF	-22.8602	22.7308
NL-means	-25.1134	23.0250
NLFMT	<b>-19.5651</b>	<b>18.7301</b>
BM3D	-11.2134	9.8694

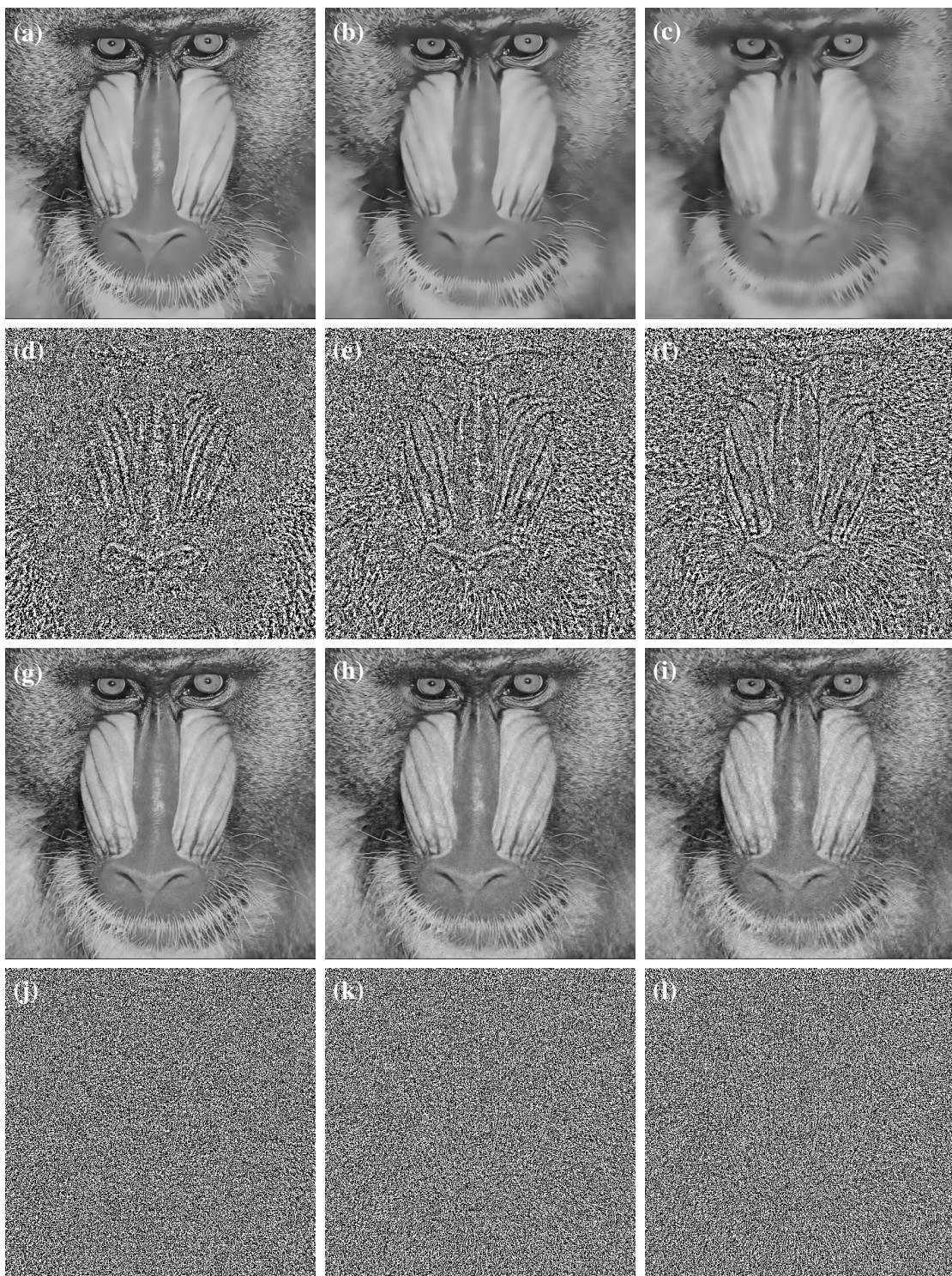


**Fig. 4** (a) - (c) denoised images by NL-means and its method noise in (d) - (f), (g) - (i) by NLFMT and its method noise in (j) - (l) with  $\sigma \in [10, 20, 30]$  respectively.

The image quality is measured by visual inspection as there is no generally accepted objective way to judge the image quality of a denoised image. There are two criteria that are used widely in the literature: (1) visibility of the artifacts, and (2) preservation of edge details. For image

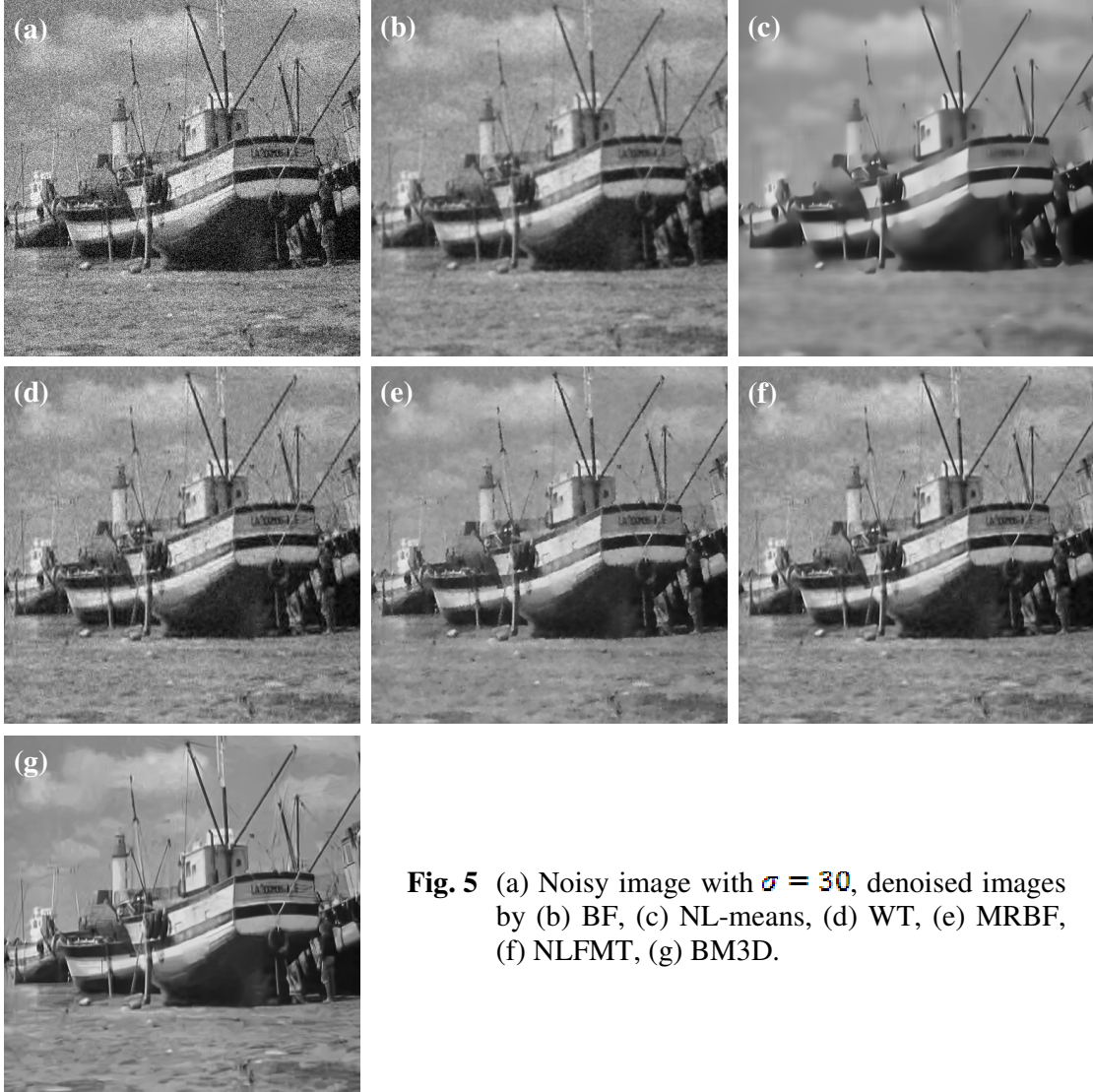


**Fig. 5** (a) Noisy image with  $\sigma = 30$ , denoised images by (b) BF, (c) NL-means, (d) WT, (e) MRBF, (f) NLFMT, (g) BM3D.

quality comparison, Lena, boat and Barbara images are considered with different  $\sigma$  to compare the performance of the proposed method with BF, NL-means, WT, MRBF and BM3D.

The denoised images of boat with  $\sigma = 30$  by different methods are shown in Fig. 5 and that of Lena with  $\sigma = 40$  in Fig. 6. In order to explain the performance of NLFMT, the selected portions of the denoised images of Lena and Barbara are considered in Figs. 7, 8 and 9. In these figures, (a) shows the noisy image, and (b), (c), (d), (e), (f) and (g) shows its denoised images by BF, NL-means, WT, MRBF, NLFMT and BM3D respectively. It is known that the BF removes noise by domain filtering and retains the edges by range filtering but this is at the cost of image details. This is observed in (b) of Figs. 5, 6, 7, 8 and 9 that the image details also have been smoothed along with the noise by domain filtering, especially in Figs. 8 (b) (top portion of the image) and 9 (b) (crosshair pattern of chair and line pattern on cloth covering the head). The application of NL-means filter removes the details to some extent and blurs the image at low SNR as the similar local patches used to find pixel weights are noisy ((c) of Figs. 5, 6, 7, 8 and 9). It is observed from (d) of Figs. 5, 6, 7, 8, 9 that the denoised images by WT still have some amount of noise with blocking artifacts and able to retain some of the details. In MRBF, the application of BF on approximation subband obtained after one level of wavelet decomposition makes to lose some of the image details present in that subband because of



**Fig. 6** (a) Noisy image with  $\sigma = 40$ , denoised images by (b) BF, (c) NL-means, (d) WT, (e) MRBF, (f) NLFMT, (g) BM3D.

domain filter inherent in BF. Further, like iterated BF, the MRBF also has the effect of flattening the gray levels in an image considerably resulting in a cartoon-like appearance [18] due to application of BF after each level of wavelet reconstruction. The flattening effect of gray levels and loss of image details can be observed in (e) of Figs. 5, 6, 7, 8 and 9. Also, it is observed that the edges look like distorted in (e) of Figs. 8 (edges of cupboard and books) and 9 (edge of chair's leg). BM3D has shown good performance in all the cases and is superior to proposed method. Eventhough the noise present in the denoised image by NLMFT is little more than that by MRBF, the performance of NLFMT is better than that of MRBF in terms of details and edges. The hat portion of the Lena image has more details in denoised image by NLFMT (Fig. 7(f)) than that by MRBF (Fig. 7 (e)). Similarly, crosshair pattern of chair and line pattern on cloth covering the head in Barbara image is clearly visible in denoised image by NLFMT (Fig. 9(f)) than that by MRBF (Fig. 9 (e)). The edges in denoised images by NLFMT are not distorted like that of MRBF ((e) and (f) of Fig. 8 and 9). From these observations it is found that, the performance of the proposed method is superior to that of WT, BF and NL-means, and is superior/similar to that of MRBF.

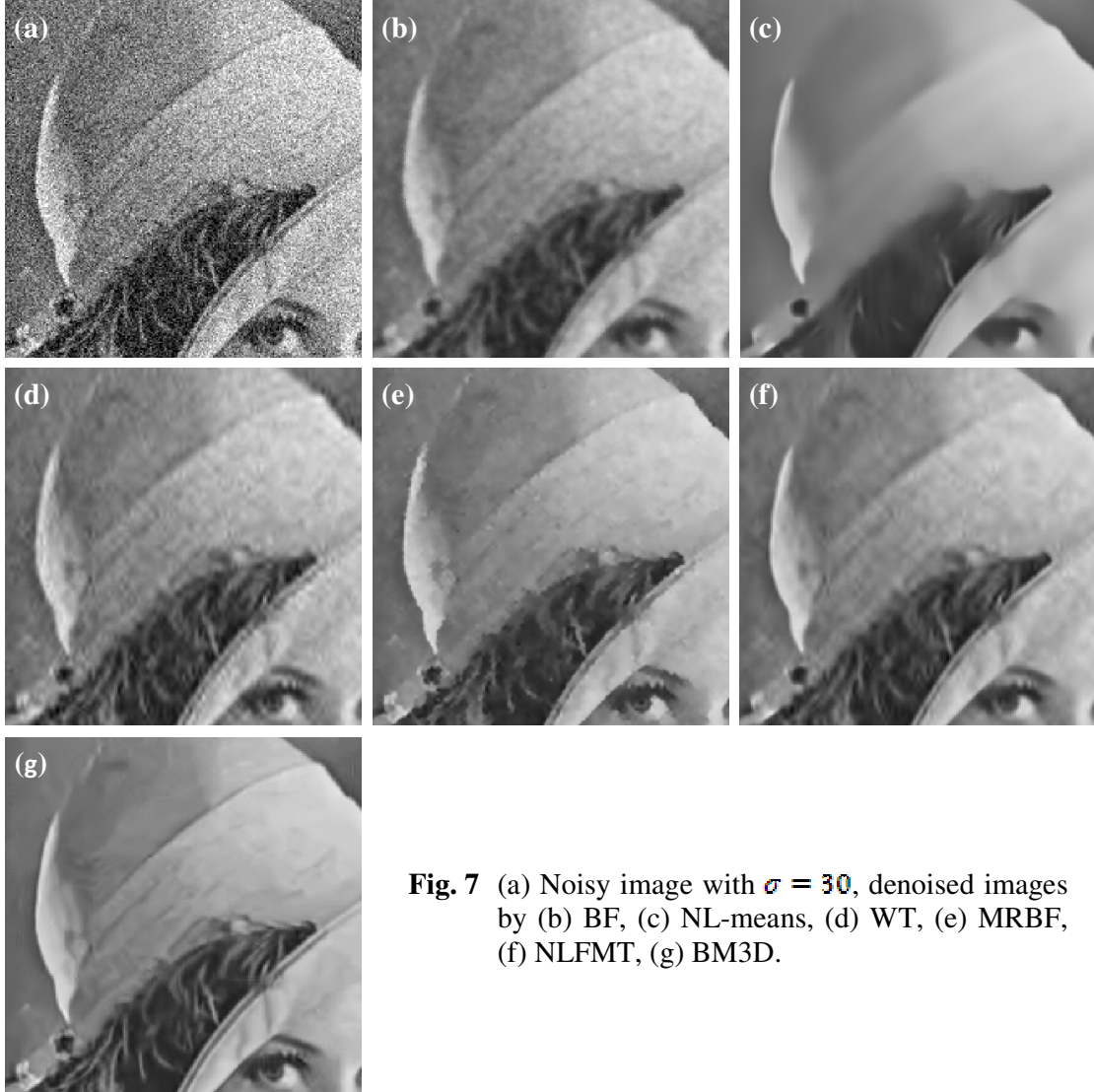


**Fig. 7** (a) Noisy image with  $\sigma = 30$ , denoised images by (b) BF, (c) NL-means, (d) WT, (e) MRBF, (f) NLFMT, (g) BM3D.

The performances of the proposed methods are measured quantitatively using PSNR and Image Quality Index (IQI) of the denoised images. The IQI of the denoised image is defined as a product of three factors: loss of correlation, luminance distortion and contrast distortion, and given as [A31]:

$$\text{IQI} = \left( \frac{\sigma_{IB}}{\sigma_I \sigma_B} \right) \left( \frac{2m_I m_B}{m_I^2 + m_B^2} \right) \left( \frac{2\sigma_I \sigma_B}{\sigma_I^2 + \sigma_B^2} \right) \quad (14)$$

$$\text{where, } m_I = \frac{1}{MN} \sum_{i=1}^M \sum_{j=1}^N I(i,j), \quad m_B = \frac{1}{MN} \sum_{i=1}^M \sum_{j=1}^N B(i,j)$$

$$\sigma_I^2 = \frac{1}{MN-1} \sum_{i=1}^M \sum_{j=1}^N (I(i,j) - m_I)^2, \quad \sigma_B^2 = \frac{1}{MN-1} \sum_{i=1}^M \sum_{j=1}^N (B(i,j) - m_B)^2$$

$$\sigma_{IB} = \frac{1}{MN-1} \sum_{i=1}^M \sum_{j=1}^N (I(i,j) - m_I)(B(i,j) - m_B)$$

The first component of Eqn. (14) represents the correlation coefficient between  $I$  and  $B$ , which measures the degree of linear correlation between  $I$  and  $B$  and its dynamic range is from  $-1$  to  $1$ . The second component measures how close the mean luminance is between  $I$  and  $B$  with a

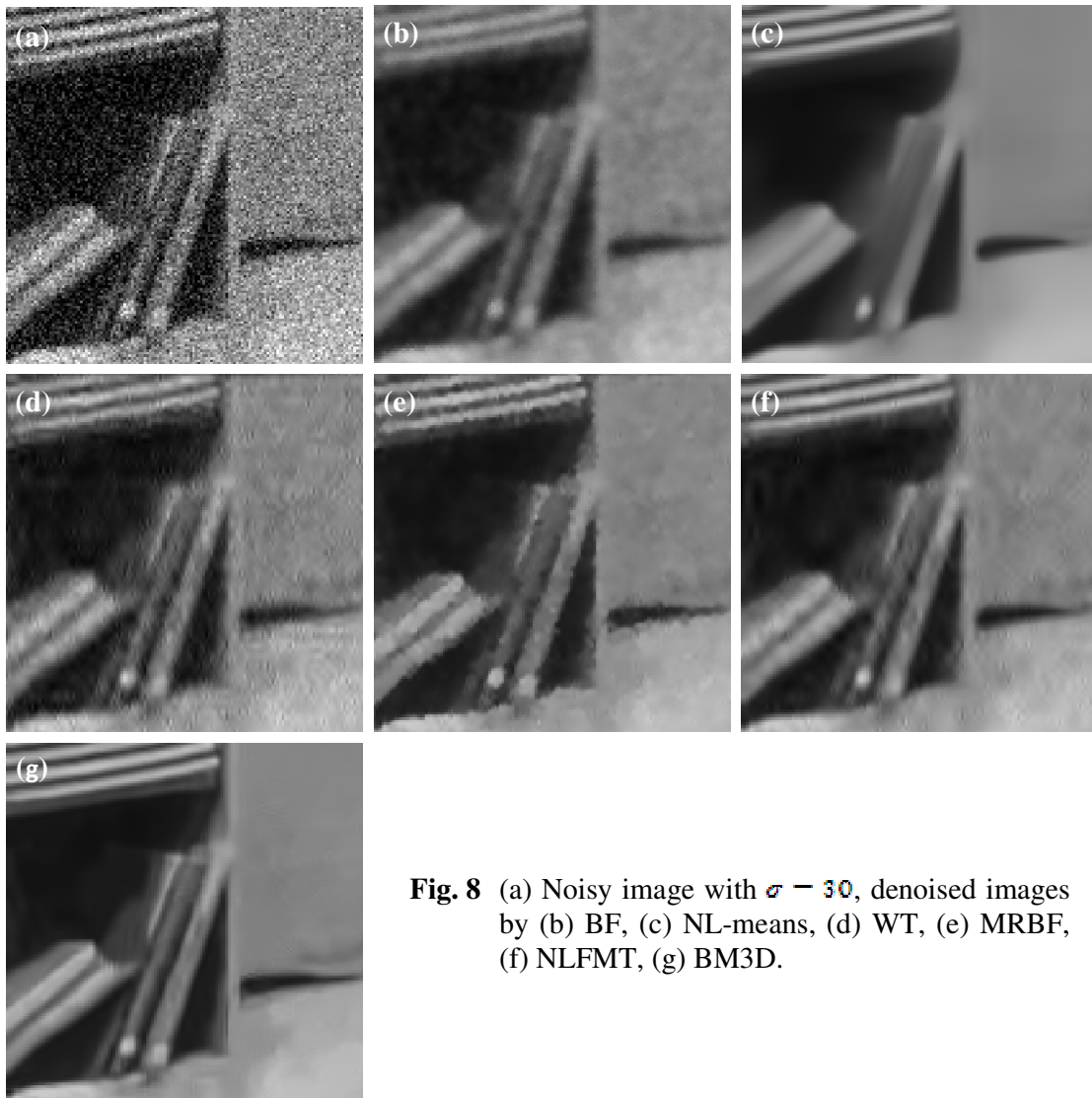


**Fig. 8** (a) Noisy image with  $\sigma = 30$ , denoised images by (b) BF, (c) NL-means, (d) WT, (e) MRBF, (f) NLFMT, (g) BM3D.

value range of  $[0, 1]$ .  $\sigma_I$  and  $\sigma_B$  can be viewed as the estimates of the contrast of  $I$  and  $B$ , so the third component with a value range of  $[0, 1]$  measures how similar the contrasts of the images are.

So, the IQI is rewritten as

$$\text{IQI} = \frac{4 m_I m_B \sigma_{IB}}{(m_I^2 + m_B^2)(\sigma_I^2 + \sigma_B^2)} \quad (15)$$

The dynamic range of IQI is  $[-1, 1]$ . The best value 1 is achieved, if and only if,  $B = I$  for all  $i = 1, 2, \dots, M$  and  $j = 1, 2, \dots, N$ . The lowest value  $-1$  occurs when  $B = 2m_I - I(i, j)$  for all  $i = 1, 2, \dots, M$  and  $j = 1, 2, \dots, N$ .

PSNR and IQI of the denoised images by different methods are tabulated in Tables 2 and 3 respectively. As BM3D has a good denoising performance, it has highest values in terms of PSNR and IQI. By excluding BM3D, the proposed methods are compared and discussed with other methods under consideration and hence the second highest PSNR and IQI values are bolded. It is observed from the Table 2 that, the denoised images by NLFMT has highest PSNR than that of other methods for images like Barbara, baboon and to some extent for Lena ( $\sigma = 10, 20$ ), boat images ( $\sigma = 10, 20$ ). The closest competitor for NLFMT is MRBF which

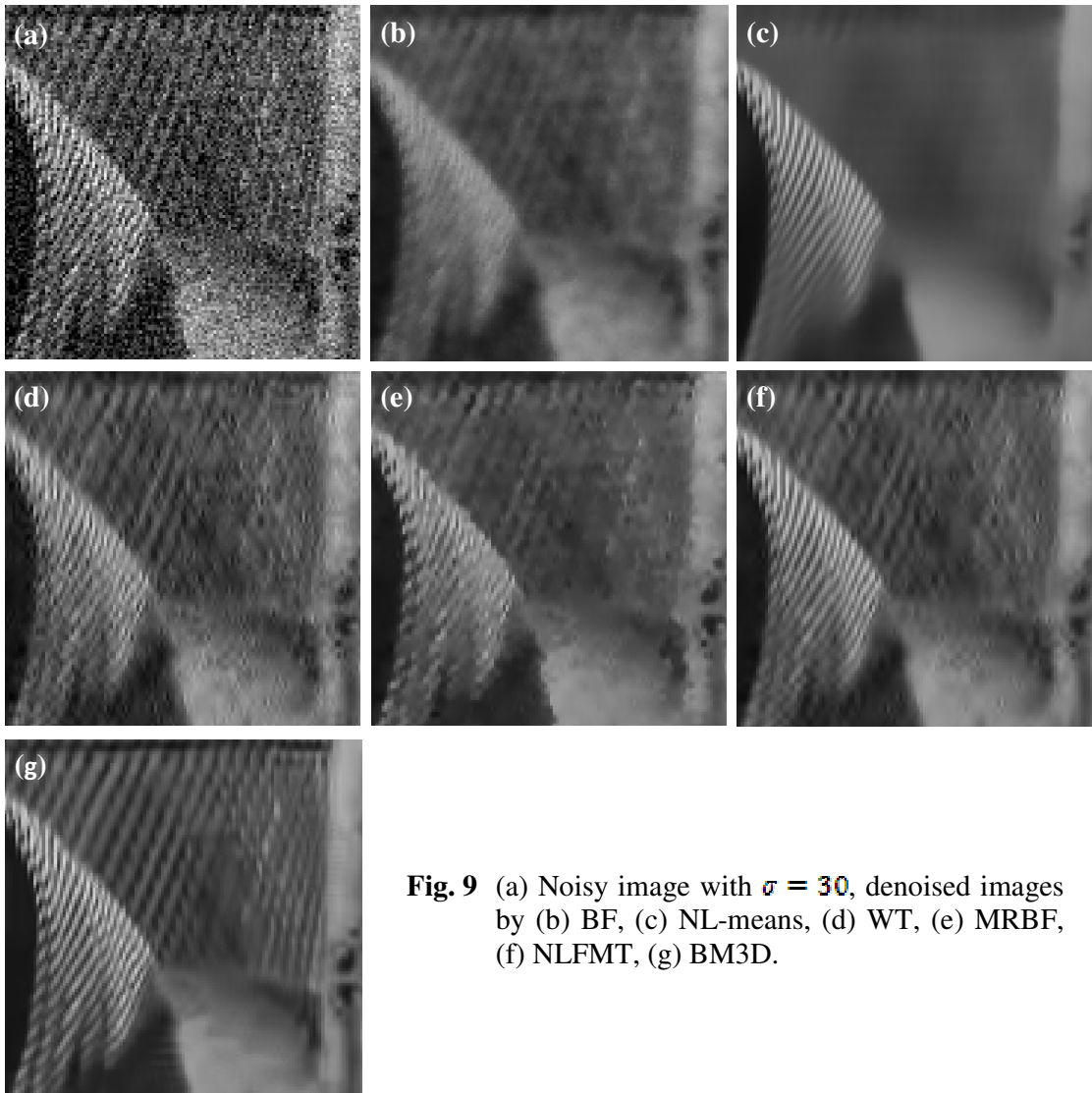


**Fig. 9** (a) Noisy image with  $\sigma = 30$ , denoised images by (b) BF, (c) NL-means, (d) WT, (e) MRBF, (f) NLFMT, (g) BM3D.

has highest PSNR for some cases of Lena ( $\sigma = 30, 40, 50$ ), boat ( $\sigma = 30, 40, 50$ ) and baboon images ( $\sigma = 50$ ). The PSNR performance of NL-means is better than BF and WT at lower  $\sigma$  and at higher  $\sigma$  either BF or WT scores over NL-means filter. From Table 3 it is noticed that, almost all the IQI values for different methods are greater than 0.9 and approaching 1. This means, when the IQI approaches 1 the denoised image is close to the original image. It is observed from Table 3 that, NLFMT has highest IQI than that of other methods for images like Barbara (all  $\sigma$ ), Lena ( $\sigma = 10, 20$ ), boat ( $\sigma = 10, 20$ ) and baboon ( $\sigma = 10, 20, 30$ ). For other  $\sigma$  of these images, MRBF scores over NLFMT in terms of IQI. Here also, IQI performance of NL-means is better than BF and WT at lower  $\sigma$  and at higher  $\sigma$  either BF or WT scores over NL-means filter. For baboon with  $\sigma = 10$ , the proposed method has higher value than that of BM3D both in terms of PSNR and IQI. From Tables 2 and 3 it is observed that, in most of the cases the denoised image with high PSNR will have higher IQI and vice versa.

Eventhough the PSNR and IQI of MRBF for boat image with  $\sigma = 30$  and Lena image with  $\sigma = 30, 40$  is greater than NLFMT, the MRBF suffers from edge distortion, detail loss and cartoon-like appearance ((e) of Figs. 5, 6 and 7). Hence, sometimes higher PSNR and IQI do not necessarily correspond to a better visual quality. In case of Barbara, the proposed NLFMT

has higher PSNR and IQI with more details and good visual quality than that of MRBF (Figs. 8 and 9). In this case, higher PSNR and IQI correspond to a better visual quality.

Table 2 PSNR of denoised images by different denoising methods

$\sigma$	10	20	30	40	50	10	20	30	40	50
<b>Input Image</b>	<b>Lena 512 x 512</b>					<b>Barbara 512 x 512</b>				
WT	33.23	29.97	28.25	27.07	26.09	31.45	27.70	25.55	24.10	23.11
MRBF	34.07	31.21	<b>29.60</b>	<b>28.31</b>	<b>27.16</b>	32.14	28.08	25.59	24.13	23.24
BF	32.01	29.70	28.43	27.39	26.40	27.32	25.04	24.24	23.65	23.09
NL-means	34.56	30.54	28.20	26.68	25.77	34.40	28.88	25.89	23.99	22.86
NLFMT	<b>35.41</b>	<b>31.62</b>	29.44	27.91	26.71	<b>35.18</b>	<b>29.96</b>	<b>26.88</b>	<b>24.84</b>	<b>23.50</b>
BM3D	35.79	32.94	31.16	29.79	28.70	35.37	32.04	29.87	27.98	26.60
<b>Input Image</b>	<b>Boat 512 x 512</b>					<b>Baboon 512 x 512</b>				
WT	31.82	28.38	26.52	25.28	24.34	29.90	25.71	23.67	22.42	21.58
MRBF	32.33	29.15	<b>27.35</b>	<b>26.13</b>	<b>25.14</b>	29.81	25.66	23.61	22.46	<b>21.76</b>
BF	29.39	27.18	26.12	25.31	24.56	25.07	23.01	22.33	21.91	21.56
NL-means	32.10	28.00	25.88	24.32	23.37	31.95	25.18	22.03	20.59	20.05
NLFMT	<b>33.47</b>	<b>29.60</b>	27.33	25.74	24.61	33.47	<b>26.94</b>	<b>24.13</b>	<b>22.58</b>	21.62
BM3D	33.86	30.81	29.01	27.60	26.38	<b>31.51</b>	27.39	25.25	23.71	22.72

Table 3 IQI of denoised images by different denoising methods

$\sigma$	10	20	30	40	50	10	20	30	40	50
<b>Input Image</b>	<b>Lena 512 x 512</b>					<b>Barbara 512 x 512</b>				
WT	0.9931	0.9875	0.9818	0.9772	0.9728	0.9880	0.9753	0.9621	0.9502	0.9410
MRBF	0.9943	0.9900	<b>0.9860</b>	<b>0.9821</b>	<b>0.9777</b>	0.9892	0.9759	0.9621	0.9508	0.9436
BF	0.9917	0.9863	0.9823	0.9779	0.9729	0.9717	0.9577	0.9513	0.9459	0.9418
NL-means	0.9951	0.9895	0.9837	0.9780	0.9728	0.9939	0.9795	0.9631	0.9471	0.9338
NLFMT	<b>0.9957</b>	<b>0.9907</b>	0.9850	0.9799	0.9749	<b>0.9944</b>	<b>0.9829</b>	<b>0.9689</b>	<b>0.9552</b>	<b>0.9445</b>
BM3D	0.9960	0.9931	0.9905	0.9879	0.9860	0.9945	0.9891	0.9840	0.9772	0.9713
<b>Input Image</b>	<b>Boat 512 x 512</b>					<b>Baboon 512 x 512</b>				
WT	0.9919	0.9825	0.9737	0.9661	0.9581	0.9827	0.9598	0.9396	0.9219	0.9073
MRBF	0.9917	0.9852	<b>0.9803</b>	<b>0.9751</b>	<b>0.9690</b>	0.9822	0.9599	0.9404	<b>0.9247</b>	<b>0.9135</b>
BF	0.9863	0.9799	0.9752	0.9696	0.9629	0.9577	0.9346	0.9243	0.9171	0.9097
NL-means	0.9893	0.9760	0.9679	0.9614	0.9536	0.9871	0.9531	0.9161	0.8856	0.8715
NLFMT	<b>0.9933</b>	<b>0.9857</b>	0.9778	0.9689	0.9596	0.9909	<b>0.9678</b>	<b>0.9447</b>	0.9241	0.9082
BM3D	0.9942	0.9886	0.9836	0.9797	0.9753	<b>0.9873</b>	0.9705	0.9551	0.9390	0.9273

It is known that, the performance of the WT based denoising method depends on the type of wavelet used. In order to analyze the effect of the same on the proposed NLFMT method, different wavelets like db8, sym8, db16, coif5, bior6.8 and DCHWT [39, 40, 41] are used to decompose the method noise. PSNR and IQI of the denoised images by NLFMT with different

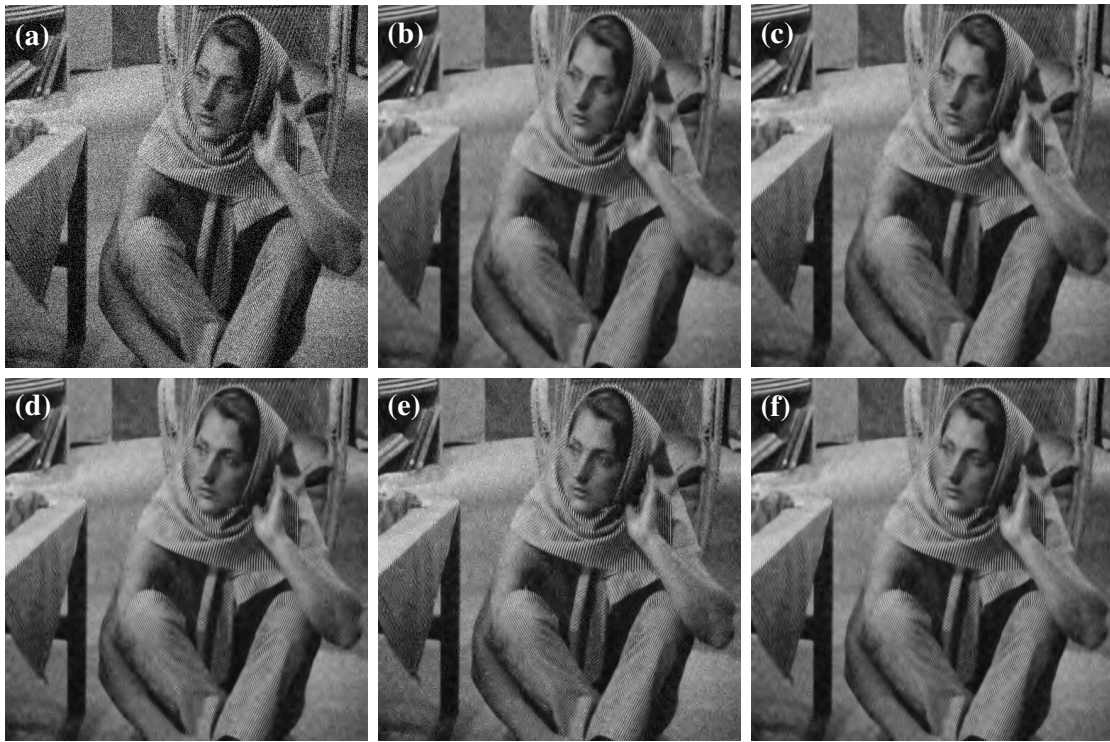
wavelets are tabulated in Tables 4 and 5 respectively. The bolded values in these tables show the highest PSNR and IQI of the denoised images by different wavelets. It is observed from the Table 4 that, the DCHWT decomposition provides highest PSNR in most of the cases and in other cases it is provided by bior6.8 and coif5. In Table 5, for most of the cases coif5 provides highest IQI and in other cases it is by DCHWT and bior6.8.

Table 4 PSNR of the denoised images by NLFMT with different wavelets by BayesShrink soft thresholding

$\sigma$	10	20	30	40	50	10	20	30	40	50
<b>Input Image</b>	<b>Lena 512 x 512</b>					<b>Barbara 512 x 512</b>				
db8	35.41	31.62	29.44	27.91	26.71	35.18	29.96	26.88	24.84	23.50
sym8	35.41	31.65	29.46	27.93	26.73	35.14	29.94	26.88	24.86	23.52
db16	35.40	31.61	29.42	27.89	26.70	35.21	29.97	26.93	24.91	23.54
coif5	35.47	31.67	<b>29.49</b>	<b>27.96</b>	26.76	35.29	30.09	27.05	25.00	<b>23.61</b>
bior6.8	<b>35.60</b>	31.49	29.11	27.44	26.14	<b>35.54</b>	30.09	26.93	24.77	23.31
DCHWT	35.47	<b>31.68</b>	29.48	<b>27.96</b>	<b>26.78</b>	35.41	<b>30.14</b>	<b>27.09</b>	<b>25.02</b>	23.60
<b>Input Image</b>	<b>Boat 512 x 512</b>					<b>Baboon 512 x 512</b>				
db8	33.47	29.60	27.32	25.74	24.61	33.47	26.94	24.13	22.58	21.62
sym8	33.43	29.63	27.33	25.78	24.65	33.51	26.93	24.13	22.57	21.60
db16	33.44	29.59	27.29	25.73	24.59	33.55	27.01	24.17	22.57	21.59
coif5	33.56	29.71	<b>27.42</b>	<b>25.87</b>	<b>24.74</b>	33.71	27.05	24.20	22.64	21.66
bior6.8	<b>33.89</b>	<b>29.76</b>	27.26	25.57	24.34	<b>34.23</b>	<b>27.46</b>	<b>24.33</b>	22.64	21.60
DCHWT	33.50	29.69	27.38	25.81	24.68	33.65	27.08	24.26	<b>22.69</b>	<b>21.73</b>

Table 5 IQI of the denoised images by NLFMT with different wavelets by BayesShrink soft thresholding

$\sigma$	10	20	30	40	50	10	20	30	40	50
<b>Input Image</b>	<b>Lena 512 x 512</b>					<b>Barbara 512 x 512</b>				
db8	<b>0.9957</b>	<b>0.9907</b>	0.9850	<b>0.9799</b>	0.9749	0.9944	0.9829	0.9689	0.9552	0.9445
sym8	0.9957	<b>0.9907</b>	0.9852	0.9798	0.9750	0.9944	0.9830	0.9691	0.9558	0.9446
db16	<b>0.9957</b>	0.9906	0.9852	<b>0.9799</b>	0.9746	0.9945	0.9833	0.9702	0.9573	0.9465
coif5	<b>0.9957</b>	0.9906	<b>0.9853</b>	0.9796	0.9742	0.9945	0.9836	<b>0.9707</b>	<b>0.9581</b>	<b>0.9475</b>
bior6.8	0.9956	0.9899	0.9833	0.9765	0.9696	<b>0.9947</b>	<b>0.9838</b>	0.9706	0.9564	0.9437
DCHWT	<b>0.9957</b>	<b>0.9907</b>	0.9852	0.9798	<b>0.9752</b>	0.9946	0.9836	0.9706	0.9574	0.9462
<b>Input Image</b>	<b>Boat 512 x 512</b>					<b>Baboon 512 x 512</b>				
db8	0.9933	0.9857	0.9778	0.9689	0.9596	0.9909	0.9678	0.9447	0.9241	0.9082
sym8	0.9931	0.9857	0.9780	0.9691	0.9605	0.9910	0.9676	0.9448	0.9240	0.9076
db16	0.9934	0.9858	0.9776	0.9683	0.9592	0.9910	0.9676	0.9445	0.9231	0.9074
coif5	0.9935	<b>0.9863</b>	<b>0.9786</b>	<b>0.9698</b>	<b>0.9611</b>	0.9913	0.9683	0.9450	0.9250	0.9089
bior6.8	<b>0.9942</b>	0.9860	0.9756	0.9646	0.9537	<b>0.9923</b>	<b>0.9709</b>	<b>0.9463</b>	0.9249	0.9076
DCHWT	0.9935	0.9862	<b>0.9786</b>	0.9696	<b>0.9611</b>	0.9912	0.9685	0.9459	<b>0.9257</b>	<b>0.9093</b>



**Fig. 10** (a) Noisy image with  $\sigma = 30$ , denoised images by NLFMT using (b) sym8, (c) db16, (d) coif5, (e) bior6.8, (f) DCHWT.

In Fig. 10, (a) shows the noisy image of Barbara with  $\sigma = 30$  and its denoised images by NLFMT using sym8, db16, coif5, bior6.8, DCHWT for method noise decomposition are shown in (b-f) respectively. It is observed from Fig. 10 that, there is a reduction of noise in all the denoised images except for a few artifacts, which are more prominent in Fig. 10 (e) (bior6.8). Further, the denoised images by sym8 (Fig. 10 (b)), coif5 (Fig. 10 (d)) and DCHWT (Fig. 10 (f)) have similar performance, and better than that of bior6.8 (Fig. 10 (e)) and db16 (Fig. 10 (c)). For Barbara image with  $\sigma = 30$ , it is observed from Tables 4 and 5 that, the NLFMT using DCHWT provides highest PSNR whereas NLFMT using coif3 provides highest IQI. Eventhough the IQI of bior6.8 is same as DCHWT; the visual quality of the denoised image using bior6.8 is not as good as that of DCHWT because of the artifacts present in that denoised image. From Fig. 10, it is observed that the denoised images by NLFMT using sym8, coif5 and DCHWT have comparable visual qualities.

## 5. CONCLUSIONS

In this paper, the amalgamation of NL-means filter and its method noise thresholding using wavelet has been proposed. The performance of the proposed methods is compared with WT based approach, BF, MRBF and NL-means filter. Through experiments conducted on standard images it was found that, the proposed method has improved the results of WT approach, BF, NL-means filter and MRBF with slight increase in performance in terms of method noise, visual quality, PSNR and IQI. Only in few cases MRBF has shown improved performance when compared to the proposed method.

The performance of the proposed method can be improved by using adaptive kernel based NL-means filter and collaborative filtering used in BM3D. Further, it is possible to improve the

results by using shift invariant wavelet transform and better subband denoising techniques for method noise decomposition and thresholding. These issues and the detailed analysis of parameter selection for the proposed framework as well as the application of other non-linear filters instead of NL-means filter are left as future work and will inspire further research towards understanding and eliminating noise in real images.

### Acknowledgements

The author would like to express his gratitude to Mr. C. R. Patil, Member (Senior Research Staff), CRL-BEL, India for his helpful and constructive comments. Also, the author would like to thank Dr. A. T. Khalghatgi, Director (R & D), BEL, India for his constant encouragement and support to carry out this work.

### REFERENCES

- [1] Gonzalez, R. C., and Woods, R. E.: Digital Image Process. Pearson Education (Singapore) Pte. Ltd., Delhi, India (2004)
- [2] Ghazel, M.: Adaptive Fractal and Wavelet Image Denoising. PhD Thesis, Department of Electrical & Computer Engineering, University of Waterloo, Ontario, Canada (2004)
- [3] Chang, S. G., Yu, B., Vetterli, M.: Adaptive Wavelet Thresholding for Image Denoising and Compression. *IEEE Trans. on Image Process.* **9**(9), 1532-1546 (2000)
- [4] Jansen, M.: Wavelet Thresholding and Noise Reduction. PhD Thesis, Department of Computer Science, Katholieke Universiteit Leuven, Heverlee, Belgium (2000)
- [5] Sendur, L., Selesnick, I. W.: Bivariate Shrinkage Functions for Wavelet-Based Denoising Exploiting Interscale Dependency. *IEEE Trans. on Signal Process.* **50**(11), 2744-2756 (2002)
- [6] Fang, H. -T., Huang, D. -S.: Wavelet De-noising by means of Trimmed Thresholding. In: Proceedings of the 5th World Congress on Intelligent Control and Automation, **2**, 1621-1624, Hangzhou, P. R. China, June (2004)
- [7] Zong, X., Laine, A. F., Geiser, E. A., Wilson, D. C.: De-Noising and Contrast Enhancement via Wavelet Shrinkage and Nonlinear Adaptive Gain. *Wavelet Applications III*. In: Proceedings of SPIE, **2762**, 566-574, Orlando, FL, April (1996)
- [8] Marpe, D., Cycon, H. L., Zander, G., Barthel, K. -U.: Context-based Denoising of Images Using Iterative Wavelet Thresholding. In: Proceedings of SPIE on Visual Communications and Image Process. **4671**, 907-914 (2002)
- [9] Cristobal, G., Cuesta, J., Cohen, L.: Image Filtering and Denoising through the Scale Transform. In: IEEE Proceedings of International Symposium on Time-Frequency and Time-Scale Analysis, 617-620, Pittsburgh, PA, October (1998)
- [10] Donoho, D. L., Johnstone, I. M.: Ideal Spatial Adaptation via Wavelet Shrinkage. *Biometrika*, **81**(3), 425-455 (1994)
- [11] Donoho, D. L.: Denoising by Soft Thresholding. *IEEE Trans. on Information Theory*, **41**(3), 613-627 (1995)
- [12] Chang, S. G., Yu, B., Vetterli, M.: Spatially Adaptive Thresholding with Context Modeling for Image Denoising, *IEEE Trans. on Image Process.* **9**(9), 1522-1531 (2000)
- [13] Pizurica, A., Philips, W.: Estimating the Probability of the Presence of a Signal of interest in Multiresolution Single and Multiband Image Denoising. *IEEE Trans on Image Process*, **15**(3), 654-665 (2006)
- [14] Bruni, V., Piccoli, B., Vitulano, D.: A Fast Computation Method for Time Scale Signal Denoising. *Signal, Image and Video Processing*, **3**(1), 63-83 (2009)

- [15] Daubechies, I.: Ten Lectures on Wavelets. In: CBMS-NSF Regional Conference Series in Applied Mathematics, SIAM, Philadelphia, USA, **61**, 2nd edition (1992)
- [16] Mallat, S.: A Wavelet Tour of Signal Processing. Academic Press, New York (1998)
- [17] Donoho, D. L., Johnstone, I. M.: Adapting to Unknown Smoothness via Wavelet Shrinkage. *Journal of the American Statistical Association*, **90**(432), 1200–1224 (1995)
- [18] Tomasi C. and Manduchi R.: Bilateral filtering for gray and color images. In: Proc. 6<sup>th</sup> Int. Conf. Computer Vision, 839–846, Bombay, India, January (1998)
- [19] Smith, S. M. and Brady, J. M.: Susan - a new approach to low level image processing. *Int. Journal of Computer Vision*, **23**(1), 45–78 (1997)
- [20] Yaroslavsky, L.: Digital Picture Processing - An Introduction. Springer Verlag (1985)
- [21] Barash, D.: A fundamental relationship between bilateral filtering, adaptive smoothing, and the nonlinear diffusion equation. *IEEE Trans. PAMI*, **24**(6), 844–847 (2002)
- [22] Elad, M.: On the origin of the bilateral filter and ways to improve it. *IEEE Trans. Image Process.* **11**(10), 1141–1151 (2002)
- [23] Morillas, S., Gregori, V. and Sapena, A.: Fuzzy bilateral filtering for color images. *Lecture Notes in Computer Science*, 138–145 (2006)
- [24] Overton, K. J. and Weymouth, T. E.: A noise reducing preprocessing algorithm. *IEEE Proc. Comput. Sci. Conf. Pattern Recognition and Image Process.* 498–507, Chicago, IL, (1979)
- [25] Perona, P. and Malik, J.: Scale-space and edge detection using anisotropic diffusion. *IEEE Trans. PAMI*, **12**(7), 629–639 (1990)
- [26] Zhang, B. and Allebach, J. P.: Adaptive bilateral filter for sharpness enhancement and noise removal. *IEEE Trans. Image Process.* **17**(5), 664–678 (2008)
- [27] Eisemann, E. and Durand, F.: Flash photography enhancement via intrinsic relighting. *Proceedings of the SIGGRAPH conference, ACM Trans. on Graphics*, **23**(3), 673–678 (2004)
- [28] Zhang, M. and Gunturk, B. K.: Multiresolution bilateral filtering for image denoising. *IEEE Trans. Image Process.* **17**(12), 2324–2333 (2008)
- [29] Wenxuan, S., Jie, L. and Minyuan, W.: An Image Denoising Method Based on Multiscale Wavelet Thresholding and Bilateral Filtering. *Wuhan University Journal of Natural Sciences*, **15**(2), 148–152 (2010)
- [30] Mustafa, Z. A. and Kadah, Y. M.: Multi Resolution Bilateral Filter for MR Image Denoising. In: Proceedings of 1<sup>st</sup> Middle East Conf. on Biomedical Engg. (MECBME), 180–184, Sharjah, UAE, February (2011)
- [31] Roy, S., Sinha, N. and Sen, A. K.: A New Hybrid Image Denoising Method. *International Journal of Information Technology and Knowledge Management*. 2(2), 491–497 (2010)
- [32] Shreyamsha Kumar, B. K.: Image Denoising based on Gaussian/Bilateral Filter and its Method Noise Thresholding. *J. SIViP* (2012). doi: 10.1007/s11760-012-0372-7
- [33] Buades A., Coll B., Morel J.: Neighborhood filters and pde's. *Numerische Mathematik*, **105**, 1–34 (2006)
- [34] Kervrann, C. and Boulanger J.: Optimal spatial adaptation for patch-based image denoising. *IEEE Trans. Image Process.* **15**(10), 2866–2878 (2006)
- [35] Xu, H., Xu, J., and Wu, F.: On the Biased Estimation of Nonlocal Means Filter. *Int. Conf. on Multimedia and Expo (ICME)*, 1149–1152, Hannover, Germany, June (2008)
- [36] Buades, A., Coll, B., and Morel, J. M.: A review of image denoising methods, with a new one. *Multiscale Modeling and Simulation*, **4**(2), 490–530 (2005).
- [37] Stein, C.: Estimation of the Mean of a Multivariate Normal Distribution. *The Annals of Statistics*, **9**(6), 1135–1151 (1981)

- [38] Dabov, K., Foi, A., Katkovnik, V., and Egiazarian, K.: Image Denoising by Sparse 3D Transform-domain Collaborative Filtering. *IEEE Trans. Image Process.* **16**(8), 2080-2095 (2007).
- [39] Shivamurti, M. and Narasimhan, S. V.: Analytic discrete cosine harmonic wavelet transform (ADCHWT) and its application to signal/image denoising. International Conf. on Signal Process. and Communications (SPCOM), 1-5, Bangalore, India, July (2010). doi: 10.1109/SPCOM.2010.5560554
- [40] Shreyamsha Kumar B.K.: Image Denoising using Discrete Cosine Harmonic Wavelets. Technical Report, Sensor Signal Process. Group, Central Research Lab. Bharat Electronics, Bangalore, Jul (2010)
- [41] Shreyamsha Kumar, B. K.: Multifocus and Multispectral Image Fusion based on Pixel Significance using Discrete Cosine Harmonic Wavelet Transform. *J. SIViP* (2012). doi: 10.1007/s11760-012-0361-x